Functional and structural neurodegenerative activities of Ankaferd BloodStopper in a mouse sciatic nerve model

RAMAZAN ÜSTÜN[1,2,], ELIF KAVAL OĞUZ[1], AYŞE ŞEKER[2] and FILIZ TASPINAR[3]

[1]Neuroscience Research Unit, School of Medicine, Van Yüzüncü Yıl University, Van 65080, Turkey;
[2]Department of Physiology, School of Medicine, Van Yüzüncü Yıl University, Van 65080, Turkey;
[3]Department of Physiology, School of Medicine, Aksaray University, Aksaray 68100, Turkey

Abstract. Traumatic and postoperative hemorrhages are life-threatening complications. Ankaferd BloodStopper (ABS) is a potent topical hemostatic agent to stop bleeding. However, ABS is associated with nerve toxicity. The present study aimed to investigate the functional and structural neurodegenerative effects of ABS in a mouse model. A total of 30 male BALB/c mice, aged 6-8 weeks, were randomly divided into control group (no treatment), a sham group (treated with saline) and an experimental group (treated with ABS). In the saline and the ABS groups, the right sciatic nerve was surgically exposed and treated with saline or ABS, respectively. No surgical procedure was performed in the control group. On day 7 post-treatment, functional changes of the sciatic nerve were evaluated by a horizontal ladder rung walking task. Structural changes were assessed with immunohistochemistry. In the horizontal ladder rung walking test, the gait impairment was proportional to the severity of sciatic nerve damage, with the ABS group showing a significantly higher rate of errors than the control and saline groups. Immunohistochemistry demonstrated extensive degeneration and deformation in the axons and myelin sheath of the sciatic nerve in the ABS group. The results provide compelling evidence for the neurotoxicity of ABS.

Introduction

Postoperative (1,2) and post-extraction bleeding in dental practice (3) are common complications in surgery. Such bleeding is easily controlled in most cases. However, the risk of bleeding during and after surgical procedures is notably increased in patients treated with antithrombotic agents (4). The application of topical hemostatic agents typically increases in clinical cases with a higher incidence of bleeding (5,6). In dentistry and medicine, Ankaferd BloodStopper (ABS; Ankaferd İlaç Kozmetik A.Ş.) has been recommended as an effective and safe alternative hemostatic agent for patients with hemostatic disorders (7-9).

ABS has been licensed as a medication to stop bleeding by the Ministry of Health of the Republic of Türkiye. ABS has been used as a topical hemostatic agent in medicine and dentistry in numerous countries, based on safety and efficacy reports indicating its sterility and non-toxicity (7). This product prevents hemorrhage in individuals with normal hemostatic parameters and patients with primary and/or secondary hemostasis (1,10). ABS is composed of five plant extracts, specifically 5 *Thymus vulgaris*, 6 *Urtica dioica*, 7 *Alpinia officinarum*, 8 *Vitis vinifera* and 9 mg *Glycyrrhiza glabra* in 100 ml Ankaferd solution (11). Each of these constituents has various effects on blood cells, angiogenesis, endothelium, cell proliferation, cell mediators and vascular dynamics. The primary action mechanism of ABS is rapidly forming an encapsulated protein network in the plasma (12). ABS has been used in dentistry (5,7) and medicine (9,13-15). To the best of our knowledge, no bleeding has been reported in patients treated with ABS.

ABS has also been used as a hemostatic agent during dental extractions in patients undergoing antithrombotic treatment with warfarin sodium and acetylsalicylic acid without interrupting anticoagulant management (16). Biological stability is essential for local hemostatic agents because they are in direct contact with periapical tissue, including soft tissue flaps, cortical and cancellous bone and peripheral nerves. Inappropriate administration of local hemostatic agents in such areas could result in adverse local tissue response and systemic complications. Therefore, the biological characteristics of local hemostatic agents must be considered, as well as their hemostatic efficacy (17).

A neuron develops a single axon that transmits electrical signals from the cell body to the target tissue over long distances (18). Peripheral nerves comprise myelinated and unmyelinated axons (19). Myelin is formed around an axon by specialized Schwann cells in the peripheral nervous system. It provides the structural basis for saltatory action potential propagation, which accelerates nerve conduction 20-100-fold compared with non-myelinated axons of the same diameter (20).

Correspondence to: Dr Ramazan Üstün, Department of Physiology, School of Medicine, Van Yüzüncü Yıl University, Campus, 3A, 10090th Street, Tusba, Van 65080, Turkey
E-mail: ramazanustun@yyu.edu.tr

Drug toxicity is known to lead to structural and functional impairments in peripheral nerves (21). Peripheral nerve damage can impair axonal connectivity by hindering cargo transport along axons or dismantling cytoskeletal structures, leading to axon loss (18). ABS is directly applied without dilution in clinical settings and the neighboring tissues are exposed to ABS for a long time (10,22). It was reported ABS causes neurotoxicity, inflammation, neurodegeneration and functional impairment in animal studies (23). Therefore, peripheral nerves exposed to ABS in clinical settings may also be at risk of degeneration.

The present study aimed to investigate the degenerative effects of ABS in a mouse sciatic nerve model. Horizontal ladder rung walking task (LRWT) was used to evaluate gait disturbance caused by nerve damage and immunohistochemistry (IHC) techniques were performed to assess pathological changes.

Materials and methods

Ethics statement. This study was conducted in compliance with Animal Research: Reporting of *In Vivo* Experiments (ARRIVE) guidelines and the relevant guidelines and regulations performed in all of the methods (24). The animal experiments were reviewed and approved by the Ethics Committee of Van Yuzuncu Yil University Laboratory Animal Center (Van, Türkiye, approval no. 27552122-604.01.02-E.696 47-2017/09).

Experimental design. A total of 30 male BALB/c mice, weighing 27-33 g and aged 6 to 8 weeks, were purchased from the Yüzüncü Yıl University Experimental Animal Production and Research Center. Mice were distributed randomly (n=10/group) into control group (no treatment), sham group (treated with saline) and experimental group (treated with ABS). The animals were housed in an air-conditioned room (21±2˚C), with a relative humidity of 45-55% and a 12:12 h light/dark cycle, with free access to food and water. All efforts were made to minimize animal suffering and reduce the number of animals used. The animals never reached the humane endpoints.

Drugs. The following drugs were used in this study: Ketamine (100 mg/ml; Hexal AG; Sandoz International GmbH), xylazine (2%; Bayer AG), saline (3 ml 0.9% sterile saline solution; Hudson RCI), Ankaferd Blood Stopper (2 ml ampoule; Trend Teknoloji İlaç AŞ).

Surgical procedure. The mice were anesthetized using 10 mg/kg xylazine intraperitoneally (i.p.) and 100 mg/kg ketamine i.p. to minimize their pain. Surgery was performed unilaterally in the right hindlimb. The sciatic nerves were exposed by making an incision in the skin and carefully separating the underlying muscles of the upper thigh. In the experimental group, 0.3 ml ABS was administered directly onto the sciatic nerve using a sterile insulin syringe. ABS was applied for 5 min and then removed by aspiration with the syringe (23). The ampoule form of ABS is used in clinical practice with 100% purity (25). Therefore, the sciatic nerves of mice were exposed to 100% ABS to mimic clinical practice.

In the sham group, 0.3 ml saline was administered instead. In the control group, no surgery was performed.

LRWT. The horizontal LRWT evaluates the walking ability of mice. It measures both forelimb and hindlimb placing, stepping and inter-limb coordination (26). The present study aimed to characterize the gait impairment of the sciatic nerve in the ABS group using the LRWT. The LRWT apparatus was adapted from the LRWT previously used in rats (26). The apparatus was composed of 2 plexiglass walls (70x16 cm). Metal rungs (2 mm diameter) were inserted to create a floor with a minimum distance of 7 mm between rungs. The ladder was elevated 11 cm above the ground. The width was 4 cm. The animals were tested on an irregular ladder pattern (random). In the irregular pattern, the distance of the rungs ranged from 0.7 to 14.0 mm. Tests were performed pre-treatment (day 0) and post-treatment (day 7). Each animal had 2 runs per session. The foot placement and walking were video-recorded from the side portion of the ladder, with a Canon EOS 750D camera (Canon Inc.) positioned at a slight ventral angle to record the experimental limb (27).

The qualitative assessment of the rear limb placement was carried out using a foot fault scoring system, as described previously (26). All video recordings were analyzed frame-by-frame, by an observer blinded to the experiments. Each step was scored according to the quality of limb placement. The following scale was used, adapted from that of Metz and Whishaw (26): 0, total miss (the limb did not touch a rung, which induced a fall; the fall disturbed the body posture and balance of the animal and stepping cycle was interrupted); 1, deep slip (limb was initially placed on a rung, then slipped off when weight-bearing, which caused the animal to fall); 2, slight slip (limb was placed on a rung and slipped; however, no fall was observed and the animal continued walking); 3, replacement (limb was placed on a rung; however, it subsequently moved to another rung); 4, correction (limb aimed for one rung; however, it was then placed on another rung without touching the first one); 5, partial placement (limb was placed on a rung with either the heel or toes; limb was fully weight bearing) and 6, correct placement (limb was placed on a rung with the palm and toes closed around it; limb was fully weight bearing) (27).

The scores and step count in each trial were calculated, and then the sum of the scores was divided by the step count. The scores of two trials were averaged for the analysis. As a result, the average gait scores of the animals were calculated.

Immunofluorescent staining. At 7 days post-treatment, animals were euthanized via decapitation under deep anesthesia by i.p. injections of xylazine (10 mg/kg) and ketamine (100 mg/kg). The sciatic nerve segment between the sciatic notch and the tibial nerve was exposed to ABS. The sciatic nerves were dissected and immediately fixed in 4% cold paraformaldehyde for 4 h at room temperature (28), then cryoprotected in 30% sucrose. The tissues were then rinsed in 0.1 M PBS three times. Next, 15-μm-thick frozen sagittal sections were cut serially at -25˚C on a Leica CM1520 cryostat (Leica Microsystems), and placed on glass slides covered with poly-L-lysine (MilliporeSigma). The sections were blocked with blocking buffer (2% BSA
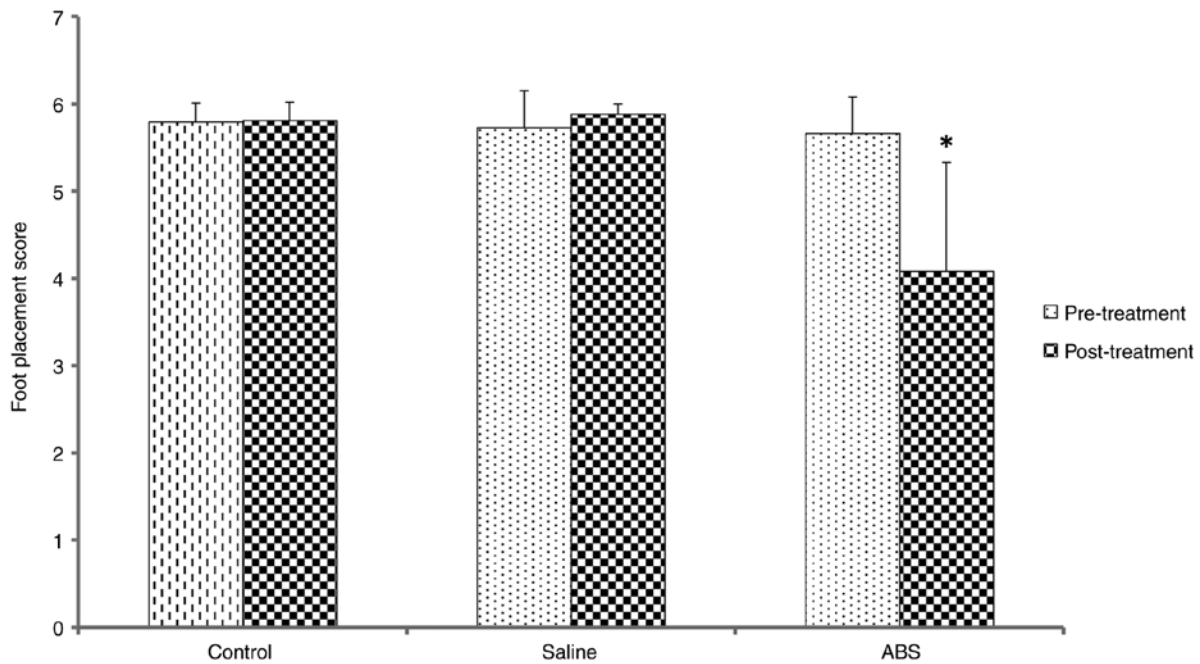
Figure 1. Topical ABS treatment on the sciatic nerve causes gait impairment. The mean stepping error score for the hind-limbs on the irregular pattern in the horizontal ladder rung walking task was assessed pre-(day 0) and post-(day 7) treatment. A score of 6 indicated correct placements. A score of 0 indicated a total miss. ABS group exhibited gait impairment with more foot faults on day 7 post-treatment. *P≤0.05 vs. ABS pre-treatment. ABS, Ankaferd BloodStopper®.

and 0.2% Triton-X100 in PBS; MilliporeSigma) for 1 h at room temperature. Sections were washed in PBS three times. Next, primary antibody incubation was performed overnight at 4˚C. The primary antibodies used were as follows: Anti-neurofilament heavy-chain 200 kDa (NF200; 1:100; mouse monoclonal; cat. no. NE14; Sigma-Aldrich; Merck KGaA), anti-class III β-tubulin (βIII-Tub; 1:100; mouse monoclonal; cat. no. TU-20; MilliporeSigma), anti-S100 (1:100; rabbit polyclonal; cat. no. Z0311; Dako; Agilent Technologies, Inc.), anti-myelin basic protein (MBP; 1:50; goat polyclonal; cat. no. sc-13912; Santa Cruz Biotechnology, Inc.) and anti-myelin protein 0 or peripheral myelin (P0; 1:50; rabbit polyclonal; cat. no. ABN363; MilliporeSigma). The tissue sections were washed three times in PBS and incubated with secondary antibodies for 2 h at 4˚C in the dark. The secondary antibodies used in were as follows: Alexa Fluor 568 goat anti-rabbit IgG and Alexa Fluor 488-goat anti-mouse IgM (both 1:200; cat. nos. A11036 and A11029, respectively; both Invitrogen; Thermo Fisher Scientific, Inc.) After the reaction, the sections were rinsed once with PBS. The slides were coverslipped and imaged using a Zeiss LSM 510 meta laser scanning confocal microscope (Carl Zeiss NTS GmbH) on an AxioVert 200M fluorescent microscope (Carl Zeiss NTS GmbH). The images were obtained using a 20X objective (28). NF200 and βIII-Tub are cytoskeleton proteins that are expressed by neurons (29). Axons were visualized employing NF200 and βIII-Tub immunofluorescence staining. S100 is a protein that is expressed by myelin-producing Schwann cells (30). Schwann cells were visualized with S100 immunofluorescence staining. P0 (a myelin marker) is a critical protein for myelin compaction and biogenesis. This protein can interact with signaling molecules, which is vital for myelination (31). The myelin was visualized by P0 and MBP immunofluorescence staining.

Image analysis was performed using Image J software (version 1.53; National Institutes of Health). Fluorescence intensity was measured for all of the biomarkers (NF200, S100, βIII-Tub, MBP, and P0) individually on the same day, choosing an intensity threshold in the NF200 channel so the axons and myelin were highlighted, corresponding to the regions of interest and immunoreactivity was quantified by their integrated intensity (28).

Statistical analysis. Descriptive statistics for the step scores are presented as the mean, standard deviation, minimum and maximum values. Two-way repeated measures analysis of variance (ANOVA) was used to compare the groups and pre/post treatments. IBM SPSS Statistics for Windows 23.0 (IBM Corp.) was used for all statistical computations. P<0.05 was considered to indicate a statistically significant difference

Results

Foot fault score. The results of the foot placement score analyses are shown in Fig. 1. Pre-treatment, the mean foot placement scores indicated that the mice carried out primarily correct placements, resulting in high scores. All animals had a healthy gait pattern. There was no significant difference between groups. Post-treatment, the control and saline group scores showed that the mice performed primarily correct placements (Videos S1 and S2, respectively). The post-treatment foot placement scores were compared with those pre-treatment for all groups. There was no significant difference between the control and saline groups. However, the ABS group made more errors in placement, resulting in low scores (Video S3). In the ABS group, mean foot placement score was significantly decreased post-treatment. In summary, ABS produced more foot placement deficit or gait impairment in the experimental limb.
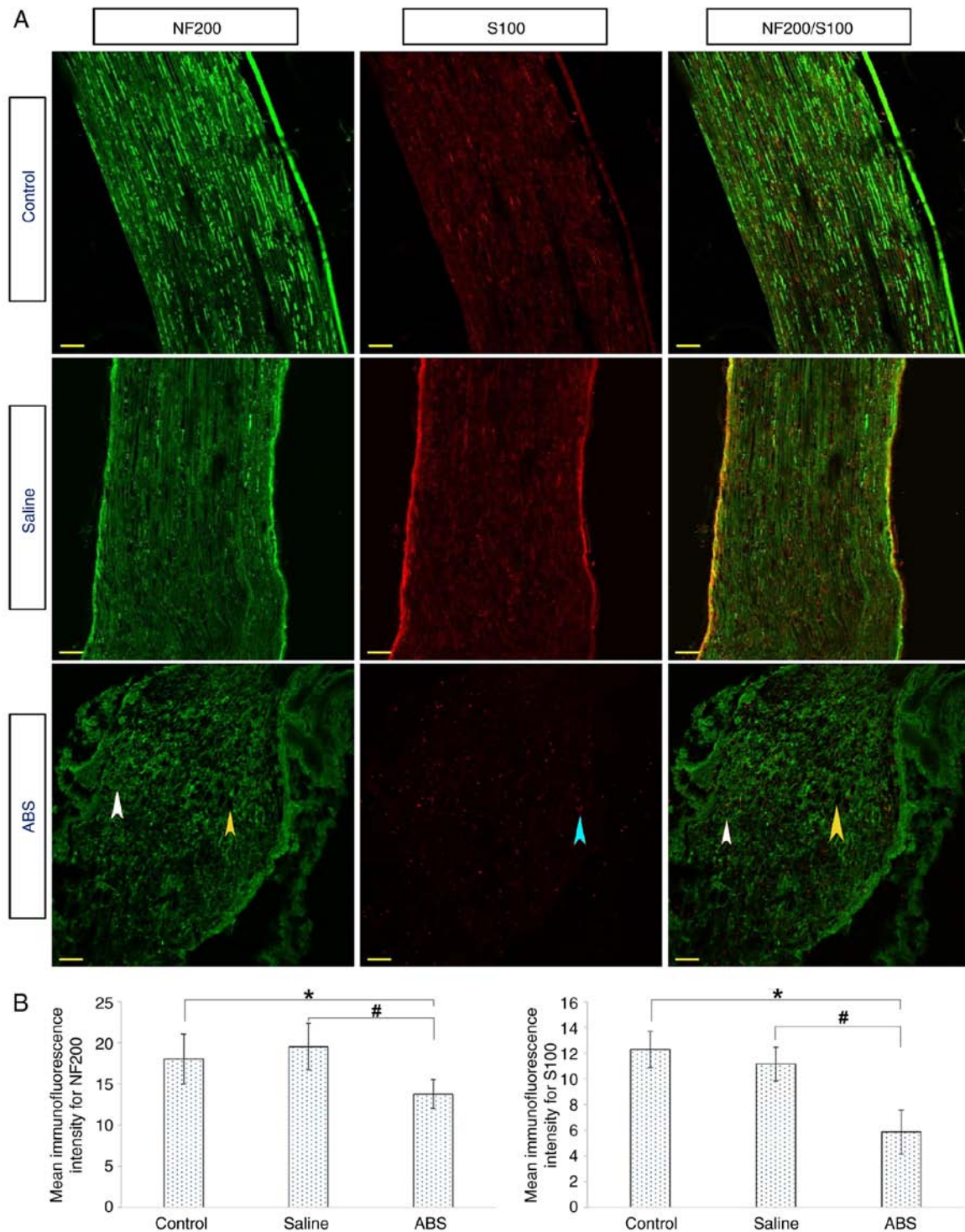
Figure 2. ABS treatment damages neuronal cytoskeleton marker NF200 and myelinating Schwann cell marker S100. (A) Longitudinal nerve sections were prepared from sciatic nerves on day 7 post-treatment. Axons were labeled with NF200 (green), and Schwann cells were marked with S100 (red). In the control and the saline groups, the NF200 and S100 were expressed at high levels by neurons and Schwann cells, respectively. However, in the ABS group, the NF200 and S100 were expressed at low levels. Laser-scanned confocal images showed that the ABS caused degeneration, deformation, degradation and fragmentation of the NF200 and S100 proteins (white and blue arrowheads, respectively). There were large cavities along the sections (yellow arrowhead). Scale bar, 50 μm. (B) Mean immunofluorescence intensities of the NF200 and S100. The ABS group showed lower fluorescence intensity than the control and saline groups. [*]P<0.05, ABS group vs. Control group; [#]P<0.05, ABS group vs. Saline group). ABS, Ankaferd BloodStopper®; NF, neurofilament.

Topical ABS treatment damages NF200 and S100. Axonal degeneration and Schwann cell destruction were evaluated by IHC. For this assay, longitudinal sections of the sciatic nerve were stained with fluorescently labeled antibodies against NF200 and S100. The representative IHC images are shown in Fig. 2A. In both the control and saline groups, NF200 (green) and S100 (red) were strong, intact and displayed regular and compact structures. Brightly labeled NF200 and S100 were observed through the longitudinal sections of the sciatic nerves. By contrast, in sciatic nerves from the ABS group, the
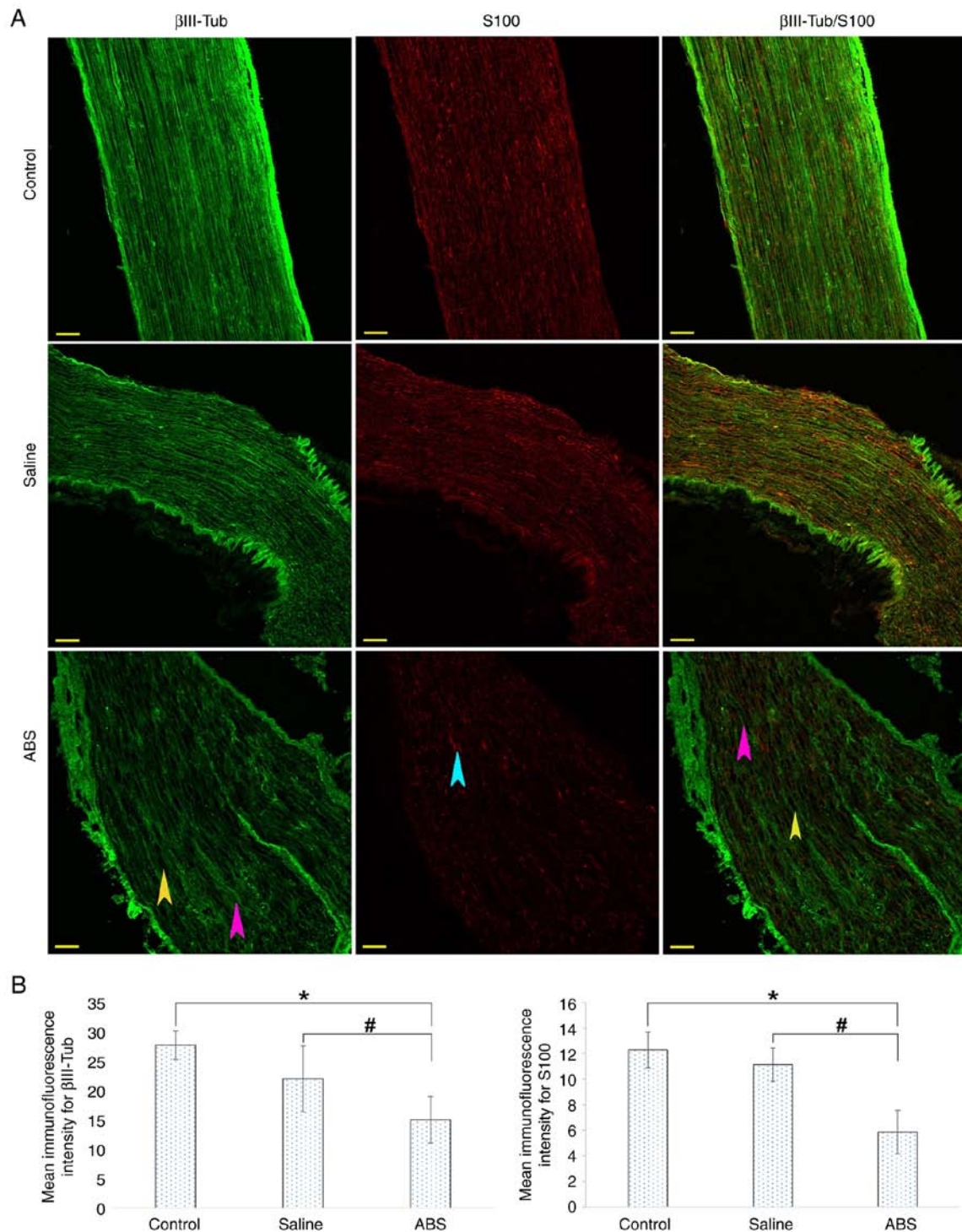
Figure 3. ABS treatment causes axonal marker βIII-Tub degeneration and deformation. (A) Axons were labeled with βIII-Tub (green) and Schwann cells were marked with S100 (red). βIII-Tub and S100 were highly expressed in the control and saline groups compared with the ABS group. However, both the βIII-Tub and S100 were expressed at low levels by the neurons in the ABS group. Control and saline groups showed regular, intact and tight cytoskeletal structures that continued along the axon. In the ABS group, however, markedly increased deformity of the βIII-Tub were observed. Furthermore, there was a loss of density and integrity of βIII-Tub (pink arrowheads). There were also large cavities (yellow arrowhead). Scale bar, 50 μm. (B) Mean immunofluorescence intensity of the βIII-Tub and S100. The ABS group showed lower fluorescence intensity than the control and saline groups. *P<0.05, ABS group vs. Control group; $^\#$P<0.05, ABS group vs. Saline group. ABS, Ankaferd BloodStopper®; βIII-Tub, Class III β-tubulin.

integrity of the NF200 degraded. The NF200 displayed an irregular and disconnected structure. In addition, cytoskeletal structure was wholly disorganized and displayed extensive cavities across the long sections. Weak red fluorescent protein (S100) showed that the Schwan cells were degenerated and decreased in number. Moreover, ABS-induced axonal damage was evaluated by assessing the immunostaining intensity (Fig. 2B). There was a significant decrease in the immunofluorescence intensities of the NF200 and S100 when the ABS group was compared with control and saline groups.
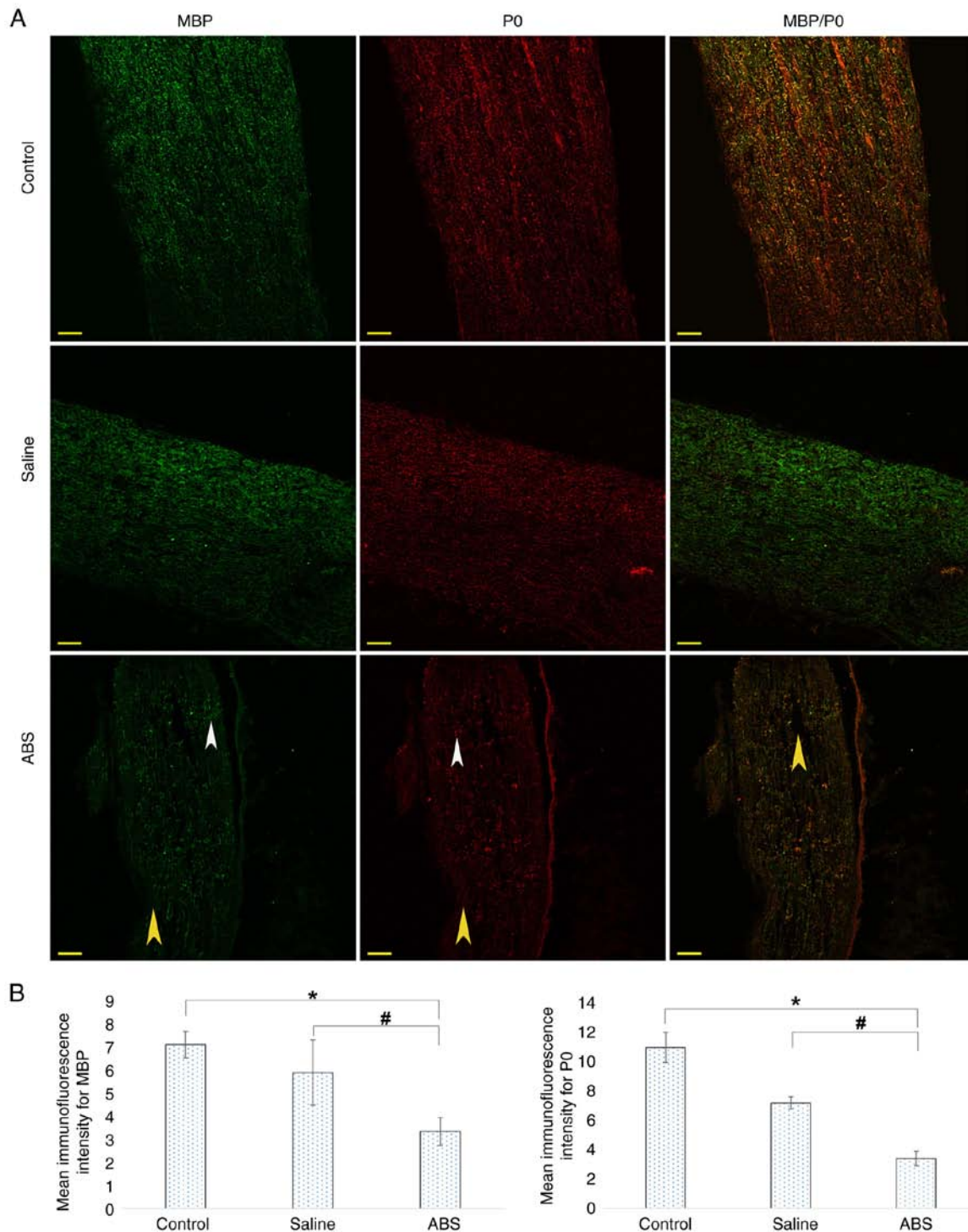
Figure 4. Topical ABS treatment induces myelin damage. (A) Myelin was labeled with MBP (green) and P0 (red). MBP and P0 were notably less expressed in the ABS group compared with control and saline groups (white arrowhead). Laser scanning confocal images of the myelin proteins (MBP and P0) showed that the control and saline groups exhibited regular myelination along the axons. ABS treatment damaged the myelin regions of the sciatic nerve (yellow arrowhead). Scale bar, 50 μm. (B) Mean immunofluorescence intensities for the MBP and P0. ABS group showed lower fluorescence intensity than the control and saline groups. The MBP and P0 had lower fluorescence intensity in the saline group compared with control group. *P<0.05, ABS group vs. Control group; #P<0.05, ABS group vs. Saline group. ABS, Ankaferd BloodStopper®; MBP, myelin basic protein; P0, myelin protein zero; βIII-Tub, Class III β-tubulin.

Topical ABS treatment deforms microtubules and alters expression of β-III-Tub. Nerve sections were stained with fluorescently labeled antibodies against βIII-Tub (green) and S100 (red). IHC images are shown in Fig. 3A. βIII-Tub in the control and saline groups showed brightly labeled regular, continuous and tight cytoskeletal structures along the axons. The S100 fluorescence indicated normal myelin-producing Schwann cell distribution. By contrast, markedly increased deformity of the βIII-Tub in the ABS group indicated disorganized and disconnected axons. Furthermore, there was a loss of density and integrity of microtubules compared with axons in the control and saline groups. There were also deep and

widespread pores. ABS-induced axonal damage was evaluated by assessing the immunostaining intensity of βIII-Tub and S100 (Fig. 3B). There was a significant decrease in the βIII-Tub and S100 immunofluorescence intensities when ABS group was compared with the control and saline groups. The βIII-Tub immunofluorescence intensity significantly decreased in the saline group compared with that in the control group.

Topical ABS treatment disrupts myelin protein. The low fluorescence intensity of the S100 suggested a substantial degeneration and loss of Schwann cells as a result of the ABS treatment. Therefore, it was investigated whether the myelin sheaths were also affected by the ABS treatment. To determine the extent of damage to the myelin sheaths, IHC was performed using antibodies against myelin-specific proteins P0 and MBP. Representative IHC images are shown in Fig. 4A. In the control and saline groups, MBP and P0 expression was evident and regularly distributed along axons, exhibiting regular myelination. Compared with control group, the ABS group displayed notable irregularity of the MBP and P0 expressions and marked deformation of the myelin structures along the axons, suggesting disrupted myelination process. In addition, there were deep and widespread pores. The ABS-induced axonal damage was evaluated by assessing the immunostaining intensity of MBP and P0 (Fig. 4B). There was a significant decrease in the MBP and P0 immunofluorescence intensity when the ABS group was compared with the control and saline groups. The MBP and P0 immunofluorescence intensity significantly decreased in the saline group compared with that in the control group.

Discussion

Previous experimental studies have suggested that ABS may have cytotoxic and degenerative effects (23,32-35). Using a sciatic nerve mouse model, the present study evaluated the potential neurodegenerative impact of ABS on peripheral nerves. The experimental design allowed evaluation of the functional and structural impacts of ABS on mouse sciatic nerve using the LRWT and IHC. The LRWT has been used as a stringent test of the sensorimotor function of rodents (36). LRWT was used to determine severity of nerve damage. The LRWT data revealed that the functional performance of sciatic nerves exposed to ABS was notably disrupted. The reduction in the foot placement score indicated damage to axons and loss of the myelin sheath around the axons. Thus, animals treated with ABS showed functional impairment. The functional results were also supported by IHC analysis.

IHC is a valuable method for demonstrating and validating impairment/damage discovered through sensorimotor function tests. IHC is an essential method as it specifically visualizes distribution and the amount of a certain molecule in the tissue using a specific antigen-antibody reaction. The use of IHC in clinical laboratories has recently expanded as more molecules involved in the pathogenesis, diagnosis, and treatment of diseases are discovered (37-39). IHC does not involve destruction of histological architecture, and thus, assessment of an expression pattern of the molecule in the microenvironment is possible (40).

Structural, functional and biomechanical integrity is key for the high conduction velocity of myelinated nerve function and axonal transport (41). The ABS group exhibited substantial degeneration and deformation as the structures of the NF200 and βIII-Tub were notably altered and displayed a loss of integrity. There were long and broad cavities along the axons. Neurofilament degradation may act as a trigger for other downstream degenerative events (42). Following axonal degeneration, Schwann cells undergo a conventional cellular program that disintegrates the myelin sheaths, a process called demyelination (43). In sciatic nerves treated with topical ABS, representative confocal images of S100 indicated that the Schwann cells were damaged and decreased in number. The achievement of peripheral nerve reconstruction and restoration relies on the ability of Schwann cells to proliferate and supply trophic support for regenerating axons (44). Within 48 h following injury, Schwann cells stop producing myelin proteins (44). In the present study, MBP and P0 were damaged and fragmented. These findings indicated myelin degeneration and fragmentation. ABS disrupted the robust myelin structure and led to fragmentation of the myelin sheaths. Both MBP and P0 are key for the maintenance of the structure of the peripheral nervous system (31). Topical ABS administration led to axonal degeneration, demyelination and decreased number of the Schwann cells. Myelin breakdown and axonal damage may alter the structure and function of peripheral nerves, which contributes to the malfunction of sensory perception and motor function (45).

Ustun and Oguz (32) showed that ABS has a degenerative effect on the peripheral sensory neurons of mice, depending on the ABS density. An *in vivo* study by Ustun *et al* measured compound muscle action potential (CMAP), motor nerve conduction velocity (MNCV), nociceptive pain sensation and motor coordination in a mouse sciatic nerve model (46). ABS treatment decreased CMAP and MNCV values, diminished the nociceptive pain sensation, weakened motor coordination and increased atrophy of the target muscles. Thus, ABS functionally led to neuromuscular impairment in mice (46). The results of the present study support the aforementioned results.

In a study by Adak *et al* (23), the left mental nerve of rats was exposed to 0.3 ml sterile saline for 5 min in the control group, while the other groups were treated with ABS, tranexamic acid and Floseal® (thrombin-containing hemostatic matrix), respectively. Following a 28-day recovery period, the nerve tissues were removed from the rats and placed in 10% formaldehyde solution for histopathological (hematoxylin & eosin, Luxol fast blue) and immunohistochemical examination. A detailed assessment was conducted on the sciatic nerve tissue, which included an evaluation of the axon structure, myelin thickness, Schwann cell count, endoneurium continuity and severity of inflammation. ABS led to a significant decrease in the number of axons and Schwann cells, decreased the myelin thickness and increased inflammation. The present study validates the histopathological results of the aforementioned study.

The neurotoxic effect on medulla spinalis of the ABS was studied histopathologically in rats by Turkoz *et al* (47). Histopathological features such as oedema, gliosis, neuronal degeneration, myelin degeneration and inflammatory cell concentration were scored as none (0), mild (1) and significant (2). ABS induced few neurologic toxicities for spinal neural

tissue. However, in the present study, the ABS led to a notable degenerative effect on the peripheral nerve. In the aforementioned study, spinal cord section was stained with hematoxylin and eosin stain and luxury fast blue stain and evaluated using a light microscope, which may not fully reflect damage to the medulla spinalis. Ultrastructural microscopic examination performed with IHC and confocal or electron microscopy, may better reflect severity and extent of neurodegeneration (48,49).

Pampu *et al* (50) performed experimental work on rat sciatic nerve with ABS. In the ABS group, 2 ml ABS was applied to the nerve region with sterile sponges for 3 min. The sponges were then removed, and NCV was assessed at 30 and 120 min and 3 weeks. A process similar to that in the ABS group was performed in the control group with sterile saline solution. According to the baseline values, the NCV values measured at different times were increased by 5% in the saline group and decreased by 20% in the ABS group. However, the difference between the ABS and saline groups was not statistically significant. The aforementioned study contradicted the results of the present research. Here, the sciatic nerve was exposed directly to pure ABS liquid for 5 min. In the aforementioned study, the sciatic nerve was in contact with an ABS-soaked sponge for 3 min. Therefore, in the present study, the sciatic nerve was more exposed to ABS; thus, greater degeneration, deformation and functional impairment occurred.

The degenerative effect of ABS on cartilage tissue and fibroblast cells has been investigated in experiments with rabbits and rats (33-35). The histopathological examination of cartilage tissue showed ABS causes fibrosis and necrosis (34,35). Mcroscopic examination of the fibroblast cells revealed decreased survival and proliferation (33). ABS may damage other tissues, such as cartilage and connective tissue, as well as peripheral nerves. Collectively, the aforementioned studies are consistent with the present findings that the application of ABS causes neurodegenerative effects in sciatic nerves.

Patients with bleeding in oral and maxillofacial surgery report numbness and dysfunction after treatment with ABS (46). The present study was designed to investigate a mouse model of the degenerative effect of ABS. The findings validate loss of sensation reported in dental practice. However, the relevance of animal studies to humans is not always clear. The present experimental data will help inform future studies related to the actual clinical practice patterns. Clinical trials will provide a clear picture of ABS-induced peripheral nerve degeneration and dysfunction in humans.

The present study focused on the effect of the ABS on the sciatic nerve. However, during ABS application, the skeletal muscles around the nerve were also exposed to the ABS. Therefore, the effect on skeletal muscles of the ABS could not be excluded. The present study focused on the neurodegenerative effects of the ABS in the acute phase (7 days post-treatment). Previous studies performed with mice have shown axonal regeneration, remyelination, and increased neuromuscular junctions 4 weeks after peripheral nerve injury (51,52). Long-term degeneration and dysfunction were not investigated at 4 weeks. Thus, we recommend repeating these tests after 4 weeks to clarify whether ABS-induced sciatic nerve degeneration is permanent and whether regeneration has started after degeneration. Persistent neurotoxic side effects of the ABS, including nerve dysfunction, diminish

patient quality of life (23,46). Another limitation of the present study is the need for deciphering peripheral nerve degeneration molecular mechanisms. It cannot be estimated which results clinical trials will produce based on sensory and motor function findings obtained from animal models. The primary limitation of this study is the lack of clinical proof of the ABS neurodegenerative effect.

The results of the present study generally support previous studies (23,32-36,46). The present study demonstrated that ABS led to the degeneration of the cytoskeletal structures of axons, fragmentation and demyelination of the myelin sheaths surrounding the axons and a decline in the number of Schwann cells, which were demonstrated by IHC. Furthermore, ABS caused dysfunction (indicated by foot placement deficits and/or gait impairment) in the sciatic nerves of mice. This dysfunction was confirmed by immunofluorescence imaging of neurodegeneration and demyelination markers. The present results indicate that the ABS can induce sensory and motor function disturbances. To prevent harm to in humans, ABS should be tested for neurotoxic and neurodegenerative effects via further experimental studies as well as clinical trials. Long-term outcomes of ABS treatment should be identified. The effect on skeletal muscle of ABS treatment should be assessed in preclinical and clinical studies. Nerve function in clinical trials is the most important outcome parameter for clinicians. Finally, the neurotoxic molecule among ABS components should be revealed.

In conclusion, the present study demonstrated that the topical application of ABS to the sciatic nerve led to notable gait impairment in the LRWT, degeneration and deformation in the axon and the myelin sheath.

Acknowledgements

Availability of data and materials

The data generated in the present study may be requested from the corresponding author.

Authors' contributions

RU conceived the study and wrote the manuscript. EO, FT and AS performed experiments. AS analyzed data and wrote the manuscript. FT and AS confirm the authenticity of all the raw data. All authors have read and approved the final version of the final manuscript.

Ethics approval and consent to participate

All experiments involving animals and surgical procedures were approved (approval no. 27552122-604.01.02-E.69647) by the Ethical Committee of University of Yüzüncü Yıl Sciences Committee in accordance with the European Community Council Directive 86/609/ECC for the care and use of laboratory animals.

Patient consent for publication

Not applicable.

Competing interests

The authors declare that they have no competing interests.

References

1. Xu B, Jin HY, Wu K, Chen C, Li L, Zhang Y, Gu WZ and Chen C: Primary and secondary postoperative hemorrhage in pediatric tonsillectomy. World J Clin Cases 9: 1543-1553, 2021.
2. von Ahnen T, Schardey J, von Ahnen M, Busch P, Schardey E, Ezzy MA, Schopf S and Wirth U: Neck circumference measurement for surveillance and early detection of hemorrhage after thyroidectomy: A diagnostic accuracy study. JAMA Otolaryngol Head Neck Surg 148: 646-653, 2022.
3. Hiroshi I, Natsuko SY, Yutaka I, Masayori S, Hiroyuki N and Hirohisa I: Frequency of hemorrhage after tooth extraction in patients treated with a direct oral anticoagulant: A multicenter cross-sectional study. PLoS One 17: e0266011, 2022.
4. Wahl MJ, Pinto A, Kilham J and Lalla RV: Dental surgery in anticoagulated patients-stop the interruption. Oral Surg Oral Med Oral Pathol Oral Radiol 119: 136-157, 2015.
5. Amer MZ, Mourad SI, Salem AS and Abdelfadil E: Correlation between International Normalized Ratio values and sufficiency of two different local hemostatic measures in anticoagulated patients. Eur J Dent 8: 475-480, 2014.
6. Keceli HG, Aylikci BU, Koseoglu S and Dolgun A: Evaluation of palatal donor site haemostasis and wound healing after free gingival graft surgery. J Clin Periodontol 42: 582-589, 2015.
7. Cakarer S, Eyupoglu E, Gunes CO, Kuseoglu BG, Berberoglu HK and Keskin C: Evaluation of the hemostatic effects of Ankaferd blood stopper during dental extractions in patients on antithrombotic therapy. Clin Appl Thromb Hemost 19: 96-99, 2013.
8. Baker RI and O'Donnell JS: How I treat bleeding disorder of unknown cause. Blood 138: 1795-1804, 2021.
9. Kar M, Cetinkaya EA and Konsuk-Unlu H: Comparison of the ankaferd blood stopper tampon and the merocel nasal tampon after septoplasty surgery. Aesthetic Plast Surg 47: 294-300, 2023.
10. Huri E, Akgul T, Ayyildiz A, Bagcioglu M and Germiyanoglu C: First clinical experience of Ankaferd BloodStopper as a hemostatic agent in partial nephrectomy. Kaohsiung J Med Sci 26: 493-495, 2010.
11. Garber A and Jang S: Novel therapeutic strategies in the management of non-variceal upper gastrointestinal bleeding. Clin Endosc 49: 421-424, 2016.
12. Iynen I, Bozkus F, San I and Alatas N: The hemostatic efficacy of Ankaferd Blood Stopper in adenoidectomy. Int J Pediatr Otorhinolaryngol 75: 1292-1295, 2011.
13. Koyuncu N: The effectiveness of ankaferd blood stopper in the management of traumatic bleeding. Adv Ther 36: 1143-1149, 2019.
14. Gilman R and Ganesh Kumar N: Invited discussion on: Comparison of the ankaferd blood stopper tampon and the merocel nasal tampon after septoplasty surgery. Aesthetic Plast Surg 47: 301-303, 2023.
15. Ozseker B, Shorbagi A, Efe C, Haznedaroglu IC and Bayraktar Y: Controlling of upper gastrointestinal bleeding associated with severe immune thrombocytopenia via topical adjunctive application of Ankaferd blood stopper. Blood Coagul Fibrinolysis 23: 464, 2012.
16. Dincol ME, Ozbas H, Yilmaz B, Ersev H, Gokyay S and Olgac V: Effect of the plant-based hemostatic agent Ankaferd Blood Stopper(R) on the biocompatibility of mineral trioxide aggregate. BMC Oral Health 16: 111, 2016.
17. Jang Y, Kim H, Roh BD and Kim E: Biologic response of local hemostatic agents used in endodontic microsurgery. Restor Dent Endod 39: 79-88, 2014.
18. Shin JE and Cho Y: Epigenetic regulation of axon regeneration after neural injury. Mol Cells 40: 10-16, 2017.
19. Sullivan R, Dailey T, Duncan K, Abel N and Borlongan CV: Peripheral nerve injury: Stem cell therapy and peripheral nerve transfer. Int J Mol Sci 17: 2101, 2016.
20. Nave KA and Werner HB: Myelination of the nervous system: Mechanisms and functions. Annu Rev Cell Dev Biol 30: 503-533, 2014.
21. Ramdharry G: Peripheral nerve disease. Handb Clin Neurol 159: 403-415, 2018.
22. Hacioglu SK, Dogu MH, Sari I and Keskin A: Successful treatment of refractory gastrointestinal bleeding by systemic (Oral) ankaferd blood stopper in a patient with glanzmann thrombasthenia. Balkan Med J 32: 218-220, 2015.
23. Adak BM, Lacin N, Simsek F, Uysal E, Soylu FE and Ozkan I: Evaluation of the effects of different hemostatic agent applications on mental nerve. Eur Arch Otorhinolaryngol 279: 5355-5362, 2022.
24. Percie du Sert N, Hurst V, Ahluwalia A, Alam S, Avey MT, Baker M, Browne WJ, Clark A, Cuthill IC, Dirnagl U, et al: The ARRIVE guidelines 2.0: Updated guidelines for reporting animal research. BMJ Open Sci 4: e100115, 2020.
25. Arslan S, Haznedaroglu IC, Öz B and Goker H: Endobronchial application of Ankaferd blood stopper to control profuse lung bleeding leading to hypoxemia and hemodynamic instability. Resp Med CME 2: 144-146, 2009.
26. Metz GA and Whishaw IQ: Cortical and subcortical lesions impair skilled walking in the ladder rung walking test: A new task to evaluate fore- and hindlimb stepping, placing, and co-ordination. J Neurosci Methods 115: 169-179, 2002.
27. Farr TD, Liu L, Colwell KL, Whishaw IQ and Metz GA: Bilateral alteration in stepping pattern after unilateral motor cortex injury: A new test strategy for analysis of skilled limb movements in neurological mouse models. J Neurosci Methods 153: 104-113, 2006.
28. Namgung U, Choi BH, Park S, Lee JU, Seo HS, Suh BC and Kim KT: Activation of cyclin-dependent kinase 5 is involved in axonal regeneration. Mol Cell Neurosci 25: 422-432, 2004.
29. Makker PG, Duffy SS, Lees JG, Perera CJ, Tonkin RS, Butovsky O, Park SB, Goldstein D and Moalem-Taylor G: Characterisation of immune and neuroinflammatory changes associated with chemotherapy-induced peripheral neuropathy. PLoS One 12: e0170814, 2017.
30. Wang Y, Li WY, Sun P, Jin ZS, Liu GB, Deng LX and Guan LX: Sciatic nerve regeneration in KLF7-transfected acellular nerve allografts. Neurol Res 38: 242-254, 2016.
31. Hao GM, Liu YG, Wu Y, Xing W, Guo SZ, Wang Y, Wang ZL, Li C, Lv TT, Wang HL, et al: The protective effect of the active components of ERPC on diabetic peripheral neuropathy in rats. J Ethnopharmacol 202: 162-171, 2017.
32. Ustun R and Oguz EK: Degenerative effect of Ankaferd Blood Stopper (R) on mice peripheral sensory neurons in vitro. Folia Neuropathol 56: 67-74, 2018.
33. Emes Y, Aybar B, Vural P, Issever H, Yalcn S, Atalay B, Dincol E and Bilir A: Effects of hemostatic agents on fibroblast cells. Implant Dent 23: 641-647, 2014.
34. Evren C, Ugur MB, Yildirim B, Bektas S, Yigit VB and Cinar F: Unpredicted effects of Ankaferd(R) on cartilage tissue. Int J Clin Exp Med 8: 922-927, 2015.
35. Kaya I, Gulabi D, Yilmaz M, Bas A, Cecen GS and Sener N: Intraarticular Ankaferd blood stopper application increases cartilagedegeneration: An experimental study. Turk J Med Sci 46: 236-240, 2016.
36. Zhang SX, Huang F, Gates M, Shen X and Holmberg EG: Early application of tail nerve electrical stimulation-induced walking training promotes locomotor recovery in rats with spinal cord injury. Spinal Cord 54: 942-946, 2016.
37. Crescenzi A and Baloch Z: Immunohistochemistry in the pathologic diagnosis and management of thyroid neoplasms. Front Endocrinol (Lausanne) 14: 1198099, 2023.
38. Harms PW, Frankel TL, Moutafi M, Rao A, Rimm DL, Taube JM, Thomas D, Chan MP and Pantanowitz L: Multiplex Immunohistochemistry and Immunofluorescence: A practical update for pathologists. Mod Pathol 36: 100197, 2023.

39. Dudas B, Lane M, Mupparaju N, Kim HM and Merchenthaler I: A forgotten principle in immunocytochemistry: Optimal dilution. J Histochem Cytochem 70: 759-765, 2022.
40. Kim SW, Roh J and Park CS: Immunohistochemistry for pathologists: Protocols, pitfalls, and tips. J Pathol Transl Med 50: 411-418, 2016.
41. Rosso G, Liashkovich I, Young P and Shahin V: Nano-scale biophysical and structural investigations on intact and neuropathic nerve fibers by simultaneous combination of atomic force and confocal microscopy. Front Mol Neurosci 10: 277, 2017.
42. Ma M, Ferguson TA, Schoch KM, Li J, Qian Y, Shofer FS, Saatman KE and Neumar RW: Calpains mediate axonal cytoskeleton disintegration during Wallerian degeneration. Neurobiol Dis 56: 34-46, 2013.
43. Tricaud N and Park HT: Wallerian demyelination: Chronicle of a cellular cataclysm. Cell Mol Life Sci 74: 4049-4057, 2017.
44. Zhou Z, Liu Y, Nie X, Cao J, Zhu X, Yao L, Zhang W, Yu J, Wu G, Liu Y and Yang H: Involvement of upregulated SYF2 in Schwann cell differentiation and migration after sciatic nerve crush. Cell Mol Neurobiol 34: 1023-1036, 2014.
45. Starobova H and Vetter I: Pathophysiology of chemotherapy-induced peripheral neuropathy. Front Mol Neurosci 10: 174, 2017.
46. Ustun R, Oguz EK, Delilbasi C, Seker A, Taspinar F, Oncu MR and Oguz AR: Neuromuscular degenerative effects of Ankaferd Blood Stopper((R)) in mouse sciatic nerve model. Somatosens Mot Res 34: 248-257, 2017.
47. Turkoz D, Demirel C, Sataloglu H and Cokluk C: Analysing the blood-stemming effect of Ankaferd Blood Stopper in medulla spinalis surgery. Turk J Med Sci 50: 1131-1135, 2020.
48. Stamm B, Moschopulos M, Hungerbuehler H, Guarner J, Genrich GL and Zaki SR: Neuroinvasion by Mycoplasma pneumoniae in acute disseminated encephalomyelitis. Emerg Infect Dis 14: 641-643, 2008.
49. Bitirgen G, Akpinar Z, Malik RA and Ozkagnici A: Use of corneal confocal microscopy to detect corneal nerve loss and increased dendritic cells in patients with multiple sclerosis. JAMA Ophthalmol 135: 777-782, 2017.
50. Pampu AA, Yildirim M, Tuzuner T, Baygin O, Abidin I, Dayisoylu EH and Senel FC: Comparison of the effects of new folkloric hemostatic agent on peripheral nerve function: An electrophysiologic study in rats. Oral Surg Oral Med Oral Pathol Oral Radiol 115: e1-e6, 2013.
51. Okuwa Y, Toriumi T, Nakayama H, Ito T, Otake K, Kurita K, Nakashima M and Honda M: Transplantation effects of dental pulp-derived cells on peripheral nerve regeneration in crushed sciatic nerve injury. J Oral Sci 60: 526-535, 2018.
52. Li L, Yokoyama H, Kaburagi H, Hirai T, Tsuji K, Enomoto M, Wakabayashi Y and Okawa A: Remnant neuromuscular junctions in denervated muscles contribute to functional recovery in delayed peripheral nerve repair. Neural Regen Res 15: 731-738, 2020.